RESEARCH ARTICLE

Endogenous automatic nerve discharge promotes nerve repair: an optimized animal model

Jing Rui[1, 2], **Ying-Jie Zhou**[1], **Xin Zhao**[1], **Ji-Feng Li**[2, 3], **Yu-Dong Gu**[1, 2], **Jie Lao**[1, 3, *]
1 Department of Hand Surgery, Huashan Hospital, Fudan University, Shanghai, China
2 Key Laboratory of Hand Reconstruction, Ministry of Health, Shanghai, China
3 Shanghai Key Laboratory of Peripheral Nerve and Microsurgery, Shanghai, China

Funding: *This study was supported by the National Natural Science Foundation of China, No. 81501051 (to JR), 81572127 (to JL); the Scientific Research Project of Huashan Hospital of Fudan University of China, No. 2013QD05 (to JR).*

Graphical Abstract

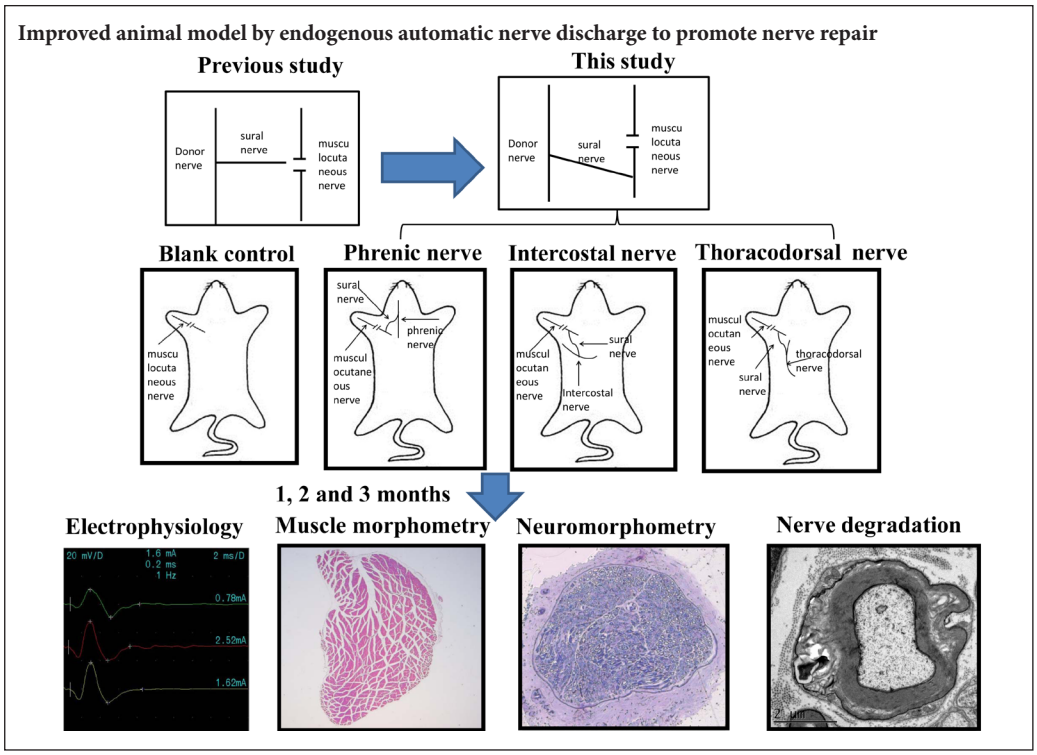

Correspondence to:
Jie Lao, MD, PhD,
laojie633@sina.com.

orcid:
0000-0003-4343-6050
(Jie Lao)

doi: *10.4103/1673-5374.244802*

Received: *January 23, 2017*
Accepted: *June 27, 2018*

Abstract

Exogenous electrical nerve stimulation has been reported to promote nerve regeneration. Our previous study has suggested that endogenous automatic nerve discharge of the phrenic nerve and intercostal nerve has a positive effect on nerve regeneration at 1 month postoperatively, but a negative effect at 2 months postoperatively, which may be caused by scar compression. In this study, we designed four different rat models to avoid the negative effect from scar compression. The control group received musculocutaneous nerve cut and repair. The other three groups were subjected to side-to-side transfer of either the phrenic (phrenic nerve group), intercostal (intercostal nerve group) or thoracodorsal nerves (thoracic dorsal nerve group), with sural nerve autograft distal to the anastomosis site. Musculocutaneous nerve regeneration was assessed by electrophysiology of the musculocutaneous nerve, muscle tension, muscle wet weight, maximum cross-sectional area of biceps, and myelinated fiber numbers of the proximal and distal ends of the anastomosis site of the musculocutaneous nerve and the middle of the nerve graft. At 1 month postoperatively, compound muscle action potential amplitude of the biceps in the phrenic nerve group and the intercostal nerve group was statistically higher than that in the control group. The myelinated nerve fiber numbers in the distal end of the musculocutaneous nerve and nerve graft anastomosis in the phrenic nerve and the intercostal nerve groups were statistically higher than those in the control and thoracic dorsal nerve groups. The neural degeneration rate in the middle of the nerve graft in the thoracic dorsal nerve group was statistically higher than that in the phrenic nerve and the intercostal nerve groups. At 2 and 3 months postoperatively, no significant difference was detected between the groups in all the assessments. These findings confirm that the phrenic nerve and intercostal nerve have a positive effect on nerve regeneration at the early stage of recovery. This study established an optimized animal model in which suturing the nerve graft to the distal site of the musculocutaneous nerve anastomosis prevented the inhibition of recovery from scar compression.

Key Words: *nerve regeneration; peripheral nerve regeneration; endogenous automatic discharge; side-to-side nerve anastomosis; phrenic nerve; intercostal nerve; animal model; electrical treatment; rats; nerve compression; neural regeneration*

Chinese Library Classification No. *R459.9; R361; R741*

Introduction

Electrical nerve stimulation has been reported to improve axon growth and is conducted as a regular treatment for peripheral nerve regeneration (Willand, 2015; Willand et al., 2015; Gordon, 2016; Gordon and English, 2016; Bueno et al., 2017). Exogenous electrical stimulation has been reported to be effective in an animal model (Al-Majed et al., 2000; Gordon, 2016) and in clinical patients with carpal tunnel syndrome, in which the stimulation improved target muscle recovery (Gordon, 2009, 2016; Gordon and English, 2016). The application of endogenous discharge, such as from the phrenic nerve and intercostal nerve, is less common than exogenous stimulation, even though the phrenic nerve (Gu et al., 1989) and intercostal nerve (Takahashi, 1983) have been used in nerve transfer for brachial plexus injury.

Compared with artificial exogenous discharge, endogenous discharge occurs inside the body under physiological conditions, and is continuous. Therefore, we thought it might also have a similar effect on nerve regeneration. Our previous study has shown that the phrenic and intercostal nerves have rhythmic clusters of discharge, which are consistent with breathing frequency (Rui et al., 2018). In the study we designed a surgical model in rat using the phrenic nerve and intercostal nerve as donor nerves. In the model, the sural nerve is autografted to connect the donor and the anastomosis site of the musculocutaneous nerve via side-to-side neurorrhaphy to maximize the neural endogenous discharge function and minimize the damage of respiratory function. The result suggested a positive effect at the early stage of recovery, but a negative effect in the middle stage, which may be caused by scar compression (Rui et al., 2018).

This study aimed to avoid the scar compression problem that happened in our previous study. We have redesigned the animal model by avoiding suturing multiple nerve ends at the same site. We have optimized the animal model to maximize the endogenous electrical stimulation and minimize the scar compression.

Materials and Methods

Animals

Seventy-two healthy, specific-pathogen-free, adult, male Sprague-Dawley rats aged approximately 6 weeks old and weighing 200 ± 10 g were provided by the Shanghai Experimental Animal Center of the Chinese Academy of Sciences, China (certificate No. SYXK (Hu) 2014-0029).

The rats were randomly divided into four groups: control group (n = 18), phrenic nerve (PN) group (n = 18), intercostal nerve (ICN) group (n = 18) and thoracic dorsal nerve (TDN) group (n = 18) (Rui et al., 2018). In each group, the rats were further randomized into three subgroups for measurement at 1, 2 and 3 months postoperatively.

The rats were housed on clean sawdust in plastic cages, with six animals per cage. They had access to food and water *ad libitum* and were housed under a 12-hour light/dark cycle. All surgery and experimental procedures were performed during the light cycle and approved by the Animal Ethics Committee of Fudan University of China (approval No. 20150628A284). All efforts were made to reduce animal numbers.

Surgical procedure

The right side was chosen as the operation side. The rats were anesthetized intraperitoneally with pentobarbital (50 mg/kg; Shanghai Reagent Company, Shanghai, China). All surgical procedures were conducted under a surgical microscope at 10× magnification. The procedure was carried out with the rat in a supine position under appropriate anesthesia at 25°C.

In the control group, the brachial plexus bundle branches were exposed in the subclavian area. The musculocutaneous nerve was identified at the terminal point into the biceps. The muscular branch was proximally exposed for 10 mm, and then transected at the middle point of the initial site and the inserting site to the biceps. The two nerve ends were directly coated with 12-0 prolene sutures tension-free (Rui et al., 2018). The skin was closed using an interrupted 5/0 silk suture.

The PN, ICN and TDN groups underwent the same basic procedure as the control group with the following additional procedures. A 2-cm-long sural nerve was harvested and used as an autograft to connect the site 5 mm distal to the musculocutaneous nerve anastomosis (**Figure 1**) and the donor nerve, PN (the PN group), the third external ICN (the ICN group) or TDN (the TDN group) by 12-0 prolene sutures tension-free (Rui et al., 2018). The epineurium of both the donor nerve and musculocutaneous nerve was removed but the perineurium was preserved at the site of coaptation. This study optimized the animal model by suturing the graft nerve 5 mm distal to the musculocutaneous nerve anastomosis instead of directly to the musculocutaneous nerve anastomosis to avoid suturing three nerve ends at the same site.

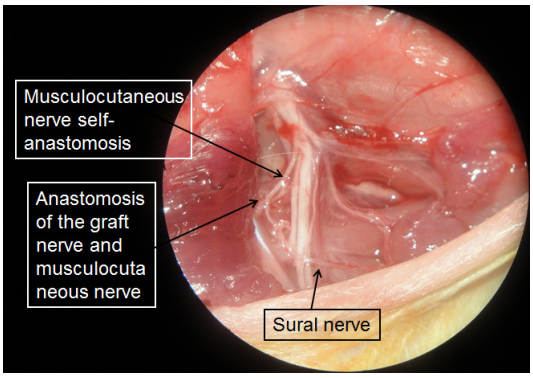

Figure 1 Intraoperative morphology of phrenic nerve, intercostal nerve, and thoracodorsal nerve under a surgical microscope at 10× magnification.
A 2-cm-long sural nerve was used as an autograft to connect the site, which was 5 mm distal to the musculocutaneous nerve anastomosis, and the donor nerve, phrenic nerve, the third external intercostal nerve or thoracic dorsal nerve for each respective group, which are not shown in this figure. The epineurium of both the donor nerve and musculocutaneous nerve were removed, but the perineurium was reserved at the site of coaptation.

Evaluation of receptor nerve recovery function

At 1, 2 and 3 months postoperatively, six rats from each group were randomly obtained using a random number generator for assessments of nerve function, including a nerve conduction study, muscle tetanic contraction force test, muscle weights, muscle histological examination, nerve histological examination and nerve fiber counting (Wang et al., 2010, 2011; Rui et al., 2012) and nerve observation with electron microscopy.

Nerve conduction study

The nerve conduction study was performed as described in our previous study (Rui et al., 2018). Briefly, the Keypoint 4 channel electrophysiological apparatus (Dantes, Skovlunde, Denmark) was used for collecting the maximum amplitude of the compound muscle action potential (CMAP), which was recorded from the right biceps muscle (Jiang et al., 2016). The operation was carefully performed to dissect the musculocutaneous nerve from the distal to proximal end and to expose the nerve terminal point into the biceps and the coaptation site, including the nerve graft and the musculocutaneous nerve anastomosis site, and the musculocutaneous nerve self-anastomosis site. An electric stimulus with a single square wave shock (2.0 mA super pulse current, 0.2 ms pulse width, 1 Hz stimulus frequency) was applied to the distal end of the nerve graft and the musculocutaneous nerve anastomosis site.

Muscle tetanic contraction force test

The tetanic force of both the ipsilateral and contralateral biceps muscles was detected by a force displacement transducer (Yang et al., 2014) (JZJ101, Chengdu Instrument, Chengdu, China) connected to a RM6240BD multichannel physiology signal collection system. The negative side (left side) was tested first. The distal portion of the biceps brachii muscle was severed at the attachment point and dissected proximally to its origin. Next, the distal stump that had been tied with a silk suture was attached to the tension transducer. After the biceps were adjusted to an optimal initial length, a train of electric stimulation was used to detect the peak amplitudes of tetanic muscle contractions. The stimulation was performed at 5 V amplitude, 100 Hz frequency, and 0.1 ms wave width with two hooked AgCl stimulating electrodes placed on the surface of the muscle. Data were recorded with an oscillograph. The muscle tetanic tension recovery rate was expressed as percentages of those obtained on the left side using the same procedure.

Muscle weights

Both sides of biceps muscles were detached from the bone at their origin and terminal point, and then weighed immediately to prevent tissue desiccation with an electronic scale (R200D, 0.0001 precision, Sartorius, Houston, TX, USA). The wet muscle weight was expressed as a percentage relative to that of the control group. The moist muscle weight recovery rate was expressed as a percentage of that on the contralateral side measured using the same procedure.

Muscle histological examination

The harvested biceps were fixed with 10% formalin, and then dehydrated in serial concentrations of alcohol and embedded by olefin. Tissue sections (5 μm thickness) from the middle of the muscles were cut and then stained with hematoxylin and eosin staining. Digital image analysis software i-solution (IMT i-Solution Inc., Vancouver, BC, Canada) was used to measure and calculate the entire cross-sectional area at a 50× magnification. The entire cross-sectional area recovery rate was expressed as a percentage of that from the contralateral side measured using the same procedure.

Nerve histological study and nerve fiber counting

The musculocutaneous nerve segment from the origin to 1 cm distal to the coaptation site was used to measure the number of nerve fibers. The specimens were fixed with 0.1 M glutaraldehyde for 4 hours (pH 7.4, 4°C) and postfixed with 2% osmium tetroxide for 2 hours, then dehydrated in serial concentrations of alcohol, and embedded in Epon. Tissue sections (0.5 μm thickness) were cut at 3 mm proximal to the musculocutaneous nerve self-anastomosis site (referred to as proximal to coaptation site) and 3 mm distal to the nerve graft and the musculocutaneous nerve anastomosis site (referred to as distal to coaptation site) of the nerve segment. Slices were stained with 5% toluidine blue, and observed by a light microscope at 200× magnification (LeicaDWLB2, Leica, Wetzlar, Germany). Five images were randomly taken from each sample by DC300F color digital camera (Leica) and analyzed by i-solution software (IMT i-Solution Inc.) (Yang et al., 2014). The total myelinated axon number was obtained by measuring the area of view and myelinated axon counts and calculating the mean density of myelinated axons.

Nerve observation with electron microscopy

Three samples from the musculocutaneous nerve segment, obtained the same way as described abovely, from each group were observed at 1 month postoperatively for ultrastructural changes by electron microscopy. The specimens were fixed with 2.5% glutaraldehyde and postfixed with 1% osmium tetroxide. The nerve samples were then dehydrated in serial concentrations of alcohol and embedded in Epon 812. Cross-sections were cut by a microtome (LKB-I, Microtome, Bromma, Sweden), and then stained with 3% uranyl acetate and lead citrate. The slices were observed and recorded using a transmission electron microscope (Philips, CM-120, Amsterdam, the Netherlands).

Evaluation of nerve graft

The myelinated axon number in the middle portion of the nerve graft (1 cm from the coaptation site) was counted under a light microscope using the same procedure as described previously. The myelinated axon in the middle portion of the nerve graft was observed under the electron microscope (Philips, CM-120). Three images were randomly taken from each sample. The degeneration rate of myelin was expressed as the percentage of the degenerating myelin

axon number to the total myelinated axon number.

Statistical analysis

All statistical analyses were performed using Prism 5.0 software (GraphPad, La Jolla, CA, USA). The data were presented as the median (25% to 75%). The Kruskal-Wallis rank test was used to compare the groups. $P < 0.05$ was considered statistically significant.

Results

Quantitative analysis of experimental animals

In total, 72 rats were involved in the trial and all were included in the final analysis without any loss. The animal model was successfully established in all rats and the surgical procedure was well tolerated. The rats in all groups survived for the duration of the experiments and no surgery-related complications or deaths occurred within the 3-month postoperatively period. All rats were measured as scheduled. No functional defects, except elbow flexion, were found after surgery.

Nerve conduction study

CMAP was recorded from biceps in all four groups while stimulating the musculocutaneous nerve at 1, 2 and 3 months postoperatively. The amplitudes in the PN and ICN groups were significantly higher than those in the control group at 1 month postoperatively ($P = 0.0115$), whereas there was no difference with the TDN group (**Figure 2A**). There was no significant difference between the four groups at 2 and 3 months postoperatively ($P = 0.6494$ and $P = 0.5171$, respectively). This result showed that at 1 month postoperatively, nerve regeneration in the PN and ICN groups had an obvious advantage compared with that in the control group, but the advantage disappeared later at 2 and 3 months postoperatively.

Muscle tension test, muscle weight and muscle histological examination

The recovery rate of tetanic tension, moist weight and entire cross-sectional area of the right biceps of the four groups increased gradually with time (**Figures 2B–D**). No significant difference was detected at 1, 2 or 3 months postoperatively between the four groups (tetanic tension: $P = 0.8857$, $P = 0.1721$, $P = 0.8222$, respectively; moist weight: $P = 0.2894$, $P = 0.0718$, $P = 0.4540$, respectively; cross-sectional area: $P = 0.3725$, $P = 0.8701$, $P = 0.5801$, respectively).

Nerve histology and nerve fiber counting

The total myelinated axon number was measured proximal to the coaptation site of the musculocutaneous nerve of the four groups at different postoperatively intervals (**Figure 2E**). No significant difference was detected between the four groups at 1, 2 and 3 months postoperatively ($P = 0.5998$, $P = 0.3984$, $P = 0.2666$, respectively).

The total myelinated axon number was also measured distal to the coaptation site of the nerve graft and musculocutaneous nerve of the four groups at different postoperatively intervals (**Figure 2F**). The axon numbers in the PN and ICN groups were significantly higher than those in the control and TDN groups at 1 month postoperatively ($P = 0.0023$). However, this difference disappeared at 2 months postoperatively due to the rapid increase of the myelinated axon number in the PN and ICN groups ($P = 0.3387$), and there was still no significant difference between the groups at 3 months postoperatively ($P = 0.9829$).

The total myelinated axon numbers were measured in the middle portion of the nerve graft of the PN, ICN, and TDN groups at different postoperative intervals (**Figure 2G**). No tendency for an increase was observed with time and no significant difference was detected between the four groups at 1, 2 and 3 months postoperatively ($P = 0.2948$, $P = 0.5655$, $P = 0.8984$, respectively).

Nerve observation with electron microscopy

At 1 month postoperatively, all regions examined (proximal to the coaptation site of the musculocutaneous nerve, distal to the coaptation site of the nerve graft and musculocutaneous nerve, and in the middle portion of the nerve graft) had similar ultrastructure to our previous study (Rui et al., 2018). Regenerated axons with a large diameter of myelination were observed proximal to the coaptation site of the musculocutaneous nerve in all four groups at 1 month post-operation, as well as newly formed and mature axons at a high magnification. However, distal to the coaptation site of the musculocutaneous nerve, a higher density of myelinated axons were observed in the PN and ICN groups compared with the TDN and negative control groups.

The degeneration rate of myelin in the middle portion of the nerve graft in the TDN group was significantly higher than that in the PN and ICN groups ($P = 0.0003$; **Figure 2H**).

Discussion

In this study, we showed that the phrenic nerve and intercostal nerve had a positive effect on nerve regeneration at 1 month postoperatively, which is consistent with the findings of our previous study (Rui et al., 2018). Further, at 2 months postoperatively, we did not observe inhibition of nerve regeneration. At 3 months postoperatively, no significant difference was detected among groups for all the parameters, as was found in our previous study.

In the previous study, we concluded that the inhibition of nerve regeneration in the middle stage may be caused by scar hyperplasia and compression due to suturing three nerve ends together. Therefore, we transferred the coaptation site from musculocutaneous nerve self-anastomosis to 5 mm distal to it. This alteration prevented the inhibition of nerve regeneration caused by scar hyperplasia and compression due to suturing multiple nerve ends together (Mafi et al., 2012; Zadegan et al., 2015), and made the nerve anastomosis closer to the target muscle (Xu et al., 2008; Yang et al., 2011; Rui et al., 2013), shortening the distance of nerve regeneration and electrical stimulation to promote nerve recovery.

CMAP and myelinated axon counts are two early stage indicators (Nichols et al., 2005; Manoli et al., 2014; Rui et

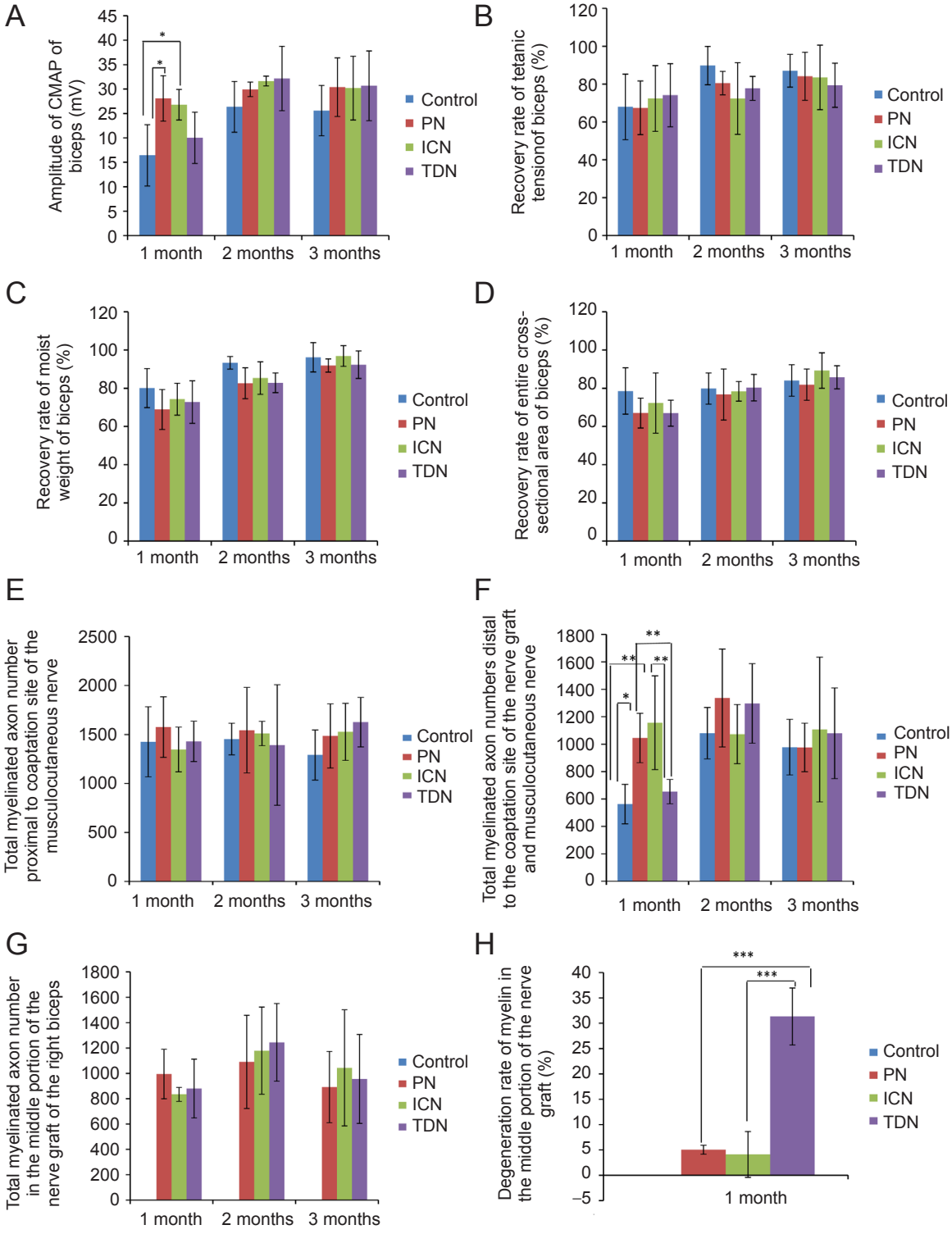

Figure 2 Different parameters in all groups at 1, 2 and 3 months postoperatively.
(A) The amplitudes of CMAP of biceps in the PN and ICN groups were significantly higher than that in the control group at 1 month postoperatively. (B–E, G) No significant difference was detected between the groups for the recovery rate of tetanic tension (B), moist weight (C) and entire cross-sectional area (D), or for total myelinated axon number proximal to coaptation site of the musculocutaneous nerve (E) and total myelinated axon number in the middle portion of the nerve graft of the right biceps (G) at 1, 2 and 3 months postoperatively. (F) The total myelinated axon numbers distal to the coaptation site of the nerve graft and musculocutaneous nerve in the PN and ICN groups were significantly higher than those in the control and TDN groups at 1 month postoperatively. (H) The degeneration rate of myelin in the middle portion of the nerve graft in the TDN group was significantly higher than that in the PN and ICN groups at 1 month postoperatively. Data are presented as the mean ± SD (Kruskal-Wallis rank test). $*P < 0.05$, $**P < 0.01$, $***P < 0.001$. CMAP: Compound muscle action potential; PN: phrenic nerve; ICN: intercostal nerve; TDN: thoracodorsal nerve.

al., 2014); thus, the increased CMAP and myelinated axon numbers in this study suggest that the phrenic nerve and intercostal nerve promoted receptor nerve regeneration by side-to-side nerve anastomosis in the early stage of recovery. The rate of myelin degeneration in the middle portion of the nerve graft indicates that nerve degeneration was mild in the phrenic and intercostal groups, which suggests that collateral sprouting (Beris and Lykissas, 2009; Bontioti and Dahlin, 2009; Tos et al., 2009) and axon regeneration might be the mechanism by which endogenous automatic nerve discharge promotes nerve repair in the early stage of recovery.

The recovery rate of tetanic tension and moist muscle weight of biceps were no longer lower in the experimental groups at the middle stage as was seen in our previous study (Rui et al., 2018), which suggests the disappearance of inhibition might be associated with the alteration of surgical procedures *via* transferring the anastomosis to the distal end to relieve the scar compression. In the late stage, no significant difference was detected between groups, similar to our previous study, which is consistent with Mackinnon's "blow-through" theory (Brenner et al., 2008; Banks et al., 2015; Lin et al., 2015). This result leads us to think that the endogenous nerve discharge probably works as a pacemaker to help the injured nerve recover within a short time. This advantage would be more obvious if the anastomosis site was farther from the target muscle. Thus, moving the anastomosis site could buy some time for the nerve recovery and reduce muscle atrophy in the clinic. The endogenous nerve discharge has great potential value in clinical application.

The mechanism of endogenous automatic nerve discharge promoting nerve regeneration may be associated with local neurotrophic factors, such as nerve growth factor and brain-derived neurotrophic factor (Hellweg and Raivich, 1994; Yin et al., 1998; Terenghi, 1999; Lykissas et al., 2007; Gordon, 2009). The biological pathway of exogenous electrical stimulation is thought to involve agitation of cAMP to promote axonal regeneration, which is the same as the latter half of the pathway in which some nerve factors promote nerve regeneration. (Gordon, 2009; Benga et al., 2017; Kolar et al., 2017; Mehrshad et al., 2017; Zuo et al., 2017). However, the mechanism of endogenous automatic nervous discharge remains unclear. In addition, further questions remain worthy of future research, including whether there is a linkage (Sherren, 1906; Babcock, 1927; Carlstedt et al., 2004) between the donor nerve and receptor nerve after side-to-side nerve anastomosis, and whether the cerebral cortex functional area would change (Jiang et al., 2010; Wang et al., 2010; Hua et al., 2012a,b, 2013) or if the functional area of donor and receptor nerves overlap.

In conclusion, we showed that the phrenic nerve and intercostal nerve showed a positive effect on the receptor nerve by side-to-side with distal nerve graft on the anastomosis side at the early stage. This optimized animal model prevented the negative effect in the middle stage due to scar compression, whereas no obvious difference was present at the late stage.

Acknowledgments: *We are thankful to our colleagues Dr. Xu, Dr. Gao, and Dr. Guan who have generously offered their assistance for trouble shooting with this work.*

Author contributions: *Study design, data analysis, trouble shooting, manuscript editing, and manuscript review: JL. Animal experiment, literature search, data acquisition, data analysis, statistical analysis, and manuscript preparation: JR. Animal experiment: YJZ. Nerve histological studies: JFL. Trouble shooting: XZ. Study design and trouble shooting: YDG. All authors approved the final version of the paper.*

Conflicts of interest: *The authors declare that there is no duality of interest associated with this manuscript.*

Financial support: *This study was supported by the National Natural Science Foundation of China, No. 81501051 (to JR), 81572127 (to JL); the Scientific Research Project of Huashan Hospital of Fudan University of China, No. 2013QD05 (to JR). The funding sources had no role in study conception and design, data analysis or interpretation, paper writing or deciding to submit this paper for publication.*

Institutional review board statement: *All experimental procedures and protocols were approved by the ethical standards of the Animal Ethics Committee of Fudan University of China (approval No. 20150628A284). All experimental procedures described here were in accordance with the National Institutes of Health (NIH) guidelines for the Care and Use of Laboratory Animals.*

Data sharing statement: *Datasets analyzed during the current study are available from the corresponding author on reasonable request.*

Plagiarism check: *Checked twice by iThenticate.*

Peer review: *Externally peer reviewed.*

Open peer reviewer: *Melanie G. Urbanchek, University of Michigan, USA.*

Additional file: *Open peer review report 1.*

References

Al-Majed AA, Neumann CM, Brushart TM, Gordon T (2000) Brief electrical stimulation promotes the speed and accuracy of motor axonal regeneration. J Neurosci 20:2602-2608.

Babcock W (1927) A standard technique for operations on peripheral nerves with especial reference to the closure of large gaps. Surg Gynecol Obstet 45:364-378.

Banks CA, Knox C, Hunter DA, Mackinnon SE, Hohman MH, Hadlock TA (2015) Long-term functional recovery after facial nerve transection and repair in the rat. J Reconstr Microsurg 31:210-216.

Benga A, Zor F, Korkmaz A, Marinescu B, Gorantla V (2017) The neurochemistry of peripheral nerve regeneration. Indian J Plast Surg 50:5-15.

Beris AE, Lykissas MG (2009) Chapter 13: Experimental results in end-to-side neurorrhaphy. Int Rev Neurobiol 87:269-279.

Bontioti E, Dahlin LB (2009) Chapter 12: Mechanisms underlying the end-to-side nerve regeneration. Int Rev Neurobiol 87:251-268.

Brenner MJ, Moradzadeh A, Myckatyn TM, Tung TH, Mendez AB, Hunter DA, Mackinnon SE (2008) Role of timing in assessment of nerve regeneration. Microsurgery 28:265-272.

Bueno CRS, Pereira M, Favaretto IAJ, Bortoluci CHF, Santos T, Dias DV, Dare LR, Rosa GMJ (2017) Electrical stimulation attenuates morphological alterations and prevents atrophy of the denervated cranial tibial muscle. Einstein (Sao Paulo) 15:71-76.

Carlstedt T, Anand P, Htut M, Misra P, Svensson M (2004) Restoration of hand function and so called "breathing arm" after intraspinal repair of C5-T1 brachial plexus avulsion injury. Case report. Neurosurg Focus 16:E7.

Gordon T (2009) The role of neurotrophic factors in nerve regeneration. Neurosurg Focus 26:E3.

Gordon T (2016) Electrical stimulation to enhance axon regeneration after peripheral nerve injuries in animal models and humans. Neurotherapeutics 13:295-310.

Gordon T, English AW (2016) Strategies to promote peripheral nerve regeneration: electrical stimulation and/or exercise. Eur J Neurosci 43:336-350.

Gu YD, Wu MM, Zhen YL, Zhao JA, Zhang GM, Chen DS, Yan JG, Cheng XM (1989) Phrenic nerve transfer for brachial plexus motor neurotization. Microsurgery 10:287-289.

Hellweg R, Raivich G (1994) Nerve growth factor: pathophysiological and therapeutic implications. Pharmacopsychiatry 27 Suppl 1:15-17.

Hua XY, Li ZY, Xu WD, Zheng MX, Xu JG, Gu YD (2012a) Interhemispheric functional reorganization after cross nerve transfer: via cortical or subcortical connectivity? Brain Res 1471:93-101.

Hua XY, Zuo CT, Xu WD, Liu HQ, Zheng MX, Xu JG, Gu YD (2012b) Reversion of transcallosal interhemispheric neuronal inhibition on motor cortex after contralateral C7 neurotization. Clin Neurol Neurosurg 114:1035-1038.

Hua XY, Liu B, Qiu YQ, Tang WJ, Xu WD, Liu HQ, Xu JG, Gu YD (2013) Long-term ongoing cortical remodeling after contralateral C-7 nerve transfer. J Neurosurg 118:725-729.

Jiang S, Li ZY, Hua XY, Xu WD, Xu JG, Gu YD (2010) Reorganization in motor cortex after brachial plexus avulsion injury and repair with the contralateral C7 root transfer in rats. Microsurgery 30:314-320.

Jiang Y, Wang L, Lao J, Zhao X (2016) Comparative study of intercostal nerve transfer to lower trunk and contralateral C7 root transfer in repair of total brachial plexus injury in rats. J Plast Reconstr Aesthet Surg 69:623-628.

Kolar MK, Itte VN, Kingham PJ, Novikov LN, Wiberg M, Kelk P (2017) The neurotrophic effects of different human dental mesenchymal stem cells. Sci Rep 7:12605.

Lin YC, Kao CH, Chen CC, Ke CJ, Yao CH, Chen YS (2015) Time-course effect of electrical stimulation on nerve regeneration of diabetic rats. PLoS One 10:e0116711.

Lykissas MG, Batistatou AK, Charalabopoulos KA, Beris AE (2007) The role of neurotrophins in axonal growth, guidance, and regeneration. Curr Neurovasc Res 4:143-151.

Mafi P, Hindocha S, Dhital M, Saleh M (2012) Advances of peripheral nerve repair techniques to improve hand function: a systematic review of literature. Open Orthop J 6:60-68.

Manoli T, Werdin F, Gruessinger H, Sinis N, Schiefer JL, Jaminet P, Geuna S, Schaller HE (2014) Correlation analysis of histomorphometry and motor neurography in the median nerve rat model. Eplasty 14:e17.

Mehrshad A, Shahraki M, Ehteshamfar S (2017) Local administration of methylprednisolone laden hydrogel enhances functional recovery of transected sciatic nerve in rat. Bull Emerg Trauma 5:231-239.

Nichols CM, Myckatyn TM, Rickman SR, Fox IK, Hadlock T, Mackinnon SE (2005) Choosing the correct functional assay: a comprehensive assessment of functional tests in the rat. Behav Brain Res 163:143-158.

Rui J, Zhao X, Zhu Y, Gu Y, Lao J (2013) Posterior approach for accessory-suprascapular nerve transfer: an electrophysiological outcomes study. J Hand Surg Eur Vol 38:242-247.

Rui J, Runge MB, Spinner RJ, Yaszemski MJ, Windebank AJ, Wang H (2014) Gait cycle analysis: parameters sensitive for functional evaluation of peripheral nerve recovery in rat hind limbs. Ann Plast Surg 73:405-411.

Rui J, Xu YL, Zhao X, Li JF, Gu YD, Lao J (2018) Phrenic and intercostal nerves with rhythmic discharge can promote early nerve regeneration after brachial plexus repair in rats. Neural Regen Res 13:862-868.

Rui J, Dadsetan M, Runge MB, Spinner RJ, Yaszemski MJ, Windebank AJ, Wang H (2012) Controlled release of vascular endothelial growth factor using poly-lactic-co-glycolic acid microspheres: in vitro characterization and application in polycaprolactone fumarate nerve conduits. Acta Biomater 8:511-518.

Sherren J (1906) Some points in the surgery of the peripheral nerves. Edinb Med J 20:297-332.

Takahashi M (1983) Studies on conversion of motor function in intercostal nerves crossing for complete brachial plexus injuries of root avulsion type. Nihon Seikeigeka Gakkai Zasshi 57:1799-1807.

Terenghi G (1999) Peripheral nerve regeneration and neurotrophic factors. J Anat 194 (Pt 1):1-14.

Tos P, Artiaco S, Papalia I, Marcoccio I, Geuna S, Battiston B (2009) Chapter 14: End-to-side nerve regeneration: from the laboratory bench to clinical applications. Int Rev Neurobiol 87:281-294.

Wang M, Li ZY, Xu WD, Hua XY, Xu JG, Gu YD (2010) Sensory restoration in cortical level after a contralateral C7 nerve transfer to an injured arm in rats. Neurosurgery 67:136-143.

Wang M, Xu W, Zheng M, Teng F, Xu J, Gu Y (2011) Phrenic nerve end-to-side neurotization in treating brachial plexus avulsion: an experimental study in rats. Ann Plast Surg 66:370-376.

Willand MP (2015) Electrical stimulation enhances reinnervation after nerve injury. Eur J Transl Myol 25:243-248.

Willand MP, Chiang CD, Zhang JJ, Kemp SW, Borschel GH, Gordon T (2015) Daily electrical muscle stimulation enhances functional recovery following nerve transection and repair in rats. Neurorehabil Neural Repair 29:690-700.

Xu WD, Lu JZ, Qiu YQ, Jiang S, Xu L, Xu JG, Gu YD (2008) Hand prehension recovery after brachial plexus avulsion injury by performing a full-length phrenic nerve transfer via endoscopic thoracic surgery. J Neurosurg 108:1215-1219.

Yang J, Chen L, Gu Y, Chen D, Wang T (2011) Selective neurotization of the radial nerve in the axilla using a full-length phrenic nerve to treat complete brachial plexus palsy: an anatomic study and case report. Neurosurgery 68:1648-1653.

Yang W, Yang J, Yu C, Gu Y (2014) End-to-side neurotization with different donor nerves for treating brachial plexus injury: an experimental study in a rat model. Muscle Nerve 50:67-72.

Yin Q, Kemp GJ, Frostick SP (1998) Neurotrophins, neurones and peripheral nerve regeneration. J Hand Surg Br 23:433-437.

Zadegan SA, Firouzi M, Nabian MH, Zanjani LO, Ashtiani AM, Kamrani RS (2015) Two-stage nerve graft in severe scar: a time-course study in a rat model. Arch Bone Jt Surg 3:82-87.

Zuo W, Wu H, Zhang K, Lv P, Xu F, Jiang W, Zheng L, Zhao J (2017) Baicalin promotes the viability of Schwann cells in vitro by regulating neurotrophic factors. Exp Ther Med 14:507-514.

P-Reviewer: Urbanchek MG; C-Editor: Zhao M; S- Editors: Wang J, Li CH; L-Editors: McCollum L, Raye W, Qiu Y, Song LP; T-Editor: Liu XL